High-performance LWIR superlattice detectors and FPA based on CBIRD design

Alexander Soibel, Jean Nguyen, Sir B. Rafol, Anna Liao, Linda Hoeglund, Arezou Khoshakhlagh, Sam A. Keo, Jason M. Mumolo, John Liu, David Z.-Y. Ting and Sarath D. Gunapala

Jet Propulsion Laboratory, California Institute of Technology, 4800 Oak Grove Dr., Pasadena, CA, 91109

ABSTRACT

We report our recent efforts on advancing of antimonide superlattice based infrared photodetectors and demonstration of focal plane arrays based on a complementary barrier infrared detector (CBIRD) design. By optimizing design and growth condition we succeeded to reduce the operational bias of CBIRD single pixel detector without increase of dark current or degradation of quantum efficiency. We demonstrated a 1024×1024 pixel long-wavelength infrared focal plane array utilizing CBIRD design. An 11.5 μm cutoff focal plane without anti-reflection coating has yielded noise equivalent differential temperature of 53 mK at operating temperature of 80 K, with 300 K background and cold-stop. Imaging results from a recent 10 μm cutoff focal plane array are also presented. These results advance state-of-the art of superlattice detectors and demonstrated advantages of CBIRD architecture for realization of FPA.

Keywords: unipolar barrier, heterostructure, infrared, photodetector, superlattice

1. INTRODUCTION

The nearly lattice-matched InAs/GaSb/AlSb (antimonide) material system offers tremendous flexibility in realizing high-performance infrared detectors. Antimonide-based superlattice (SL) detectors [1] can be tailor-made to have cutoff wavelengths ranging from the short wave infrared (SWIR) to the very long wave infrared (VLWIR). These detectors are predicted to have suppressed Auger recombination rates[2,3] and low interband tunneling,[4,5] resulting in the suppressed dark currents. Moreover, the nearly lattice-matched antimonide material system, consisting of InAs, GaSb, AlSb and their alloys, allows for the construction of superlattice heterostructures. In particular, unipolar barriers, which blocks one carrier type without impeding the flow of the other, have been implemented in the design of SL photodetectors to realize complex heterodiodes with improved performance. Heterostructure superlattice detectors that make effective use of unipolar barriers have demonstrated strong reduction of generation-recombination (G-R) dark current due to Shockley-Read-Hall (SRH) processes. Despite relatively short lifetimes found in present day superlattice material, the higher absorber doping levels afforded by immunity to tunneling has led to reduced diffusion dark current. The dark current characteristics of type-II superlattice based single element LWIR detectors are now approaching that of the state-of-the-art MCT detector. However, noise measurements highlight the need for surface leakage suppression, which can be tackled by improved etching, passivation, and device design. The various aspects of type-II superlattice infrared detectors have been covered in detail in review articles by Fuchs *et al*. [6], Bürkle and Fuchs [7], Razeghi and Mohseni [8], and Ting *et al*. [9], as well as in the book by Rogalski [10]. In this paper, we discuss some recent development in the area of type-II superlattice based infrared detectors at the Jet Propulsion Laboratory (JPL).

*Alexander.Soibel@jpl.nasa.gov; phone 818 393 0225; fax: 818 393 4540;

2. THE COMPLEMENTARY BARRIER INFRARED DETECTOR

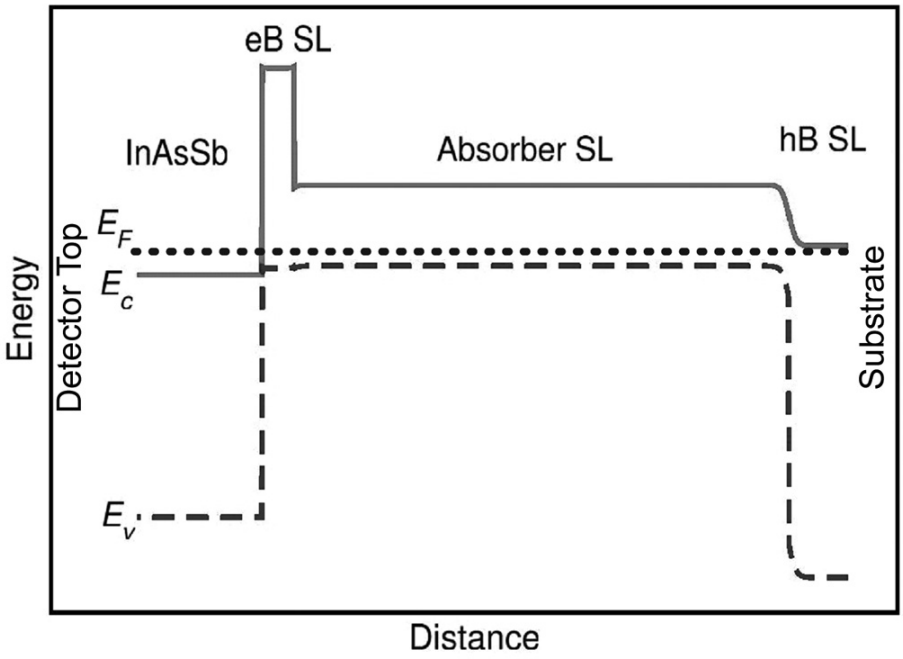

Figure 1. Calculated zero-bias energy band diagram of a complementary barrier infrared detector (CBIRD) structure, where a long-wave infrared InAs/GaSb superlattice absorber is surrounded by an InAs/AlSb superlattice hole-blocking (hB) unipolar barrier and a shorter period InAs/GaSb superlattice superlattice electron-blocking (eB) unipolar barrier.

The CBIRD design, consists of an InAs/GaSb absorber SL sandwiched between an InAs/AlSb unipolar hole barrier (hB) SL, and an InAs/GaSb unipolar electron barrier (eB) SL. Figure 1 shows calculated energy band diagrams of the CBIRD device. We expect the InAs/GaSb LWIR SL to have more favorable electron transport properties. Therefore the absorber superlattice is doped lightly p-type so that we have better minority carrier (electron) mobility. A full description of the device structure is published elsewhere.[11] The device structure was grown on GaSb (100) substrate by molecular beam epitaxy (MBE). Standard contact mode optical lithography was used to fabricated large-area (220×220 μm^2 in size) devices for dark current and responsivity measurements. Detailed device results have been reported earlier [11]. Here we summarize the key points.

In the device reported in Reference 11, we observed that the photoresponse increases with bias from 0 to ~0.2 V, and then plateaus for bias greater than 0.2 V. The 77 K dark current density at 0.2 V is still quite low, with a value of ~1×10^{-5} A/cm^2. Arrhenius plot shows that at 0.2 V, the dark current is diffusion limited for device temperature above ~77K. Spectral response measured under 0.2 V applied bias at 77 K shows that the device has a 10 μm cutoff (defined by 50% peak responsivity), with a peak responsivity of 1.5 A/W. We calculated the shot-noise limited black-body D^*, where the noise spectrum is determined by the measured dark current and photocurrent integrated over the 8 μm to 10 μm spectral range (the overlap between the atmospheric window and the detector cutoff). Under 0.2 V, the detector reaches 300 K BLIP operation at 86 K with a black-body BLIP D^* value of 1.1×10^{11} cm-Hz$^{1/2}$/W for f/2 optics. For 300K background with 2π field of view, the device shows a BLIP temperature of 101 K with a black-body BLIP D^* value of 2.6×10^{10} cm-Hz$^{1/2}$/W. The device has a zero-bias dynamic resistance-area product of R_0A =14,000 ohm-cm^2 at 77 K. However, since the detector is expected to operate at a higher bias (~0.2 V), a more relevant quantities is the effective resistance-area product, given by $RA_{\text{eff}} = kT/qJ_d$. Under a 0.2 V bias, the RA_{eff} for this device is 670 ohm-cm^2 at 77 K.

Optical characterization tools are invaluable in the study of the material properties of CBIRD detectors. We have been investigating CBIRD devices using two different optical characterization techniques: photoluminescence (PL) and transmission spectroscopy. We find that the absorption quantum efficiency (QE), deduced from the transmission measurements, served as a good estimate of the upper limit of the external QE, and the PL peak position was shown to correlate well with the detector cut-off wavelength. In a comparison between the PL intensity and the dark current characteristics, a good correlation between a high PL intensity and low dark current was observed, showing that the PL intensity well reflects the material quality. Also, SRH processes were identified as the limiting factor of the minority carrier lifetime of the CBIRD material studied. More details of these optical characterization results can be found in Reference 12.

We have also experimentally investigated the noise and gain of high-performance LWIR superlattice photodetectors. We compare the recently demonstrated SL heterodiode, which exhibits an electrical gain much larger than unity, with a SL photodetector without gain to show that the electrical gain in these devices originates from the device structure rather than from the superlattice absorber. We directly measure the noise spectra of high performance superlattice photodiodes, and demonstrated that intrinsically SL photodetectors do not exhibit 1/*f* noise. At the same time, our measurements clearly show that sidewall leakage current not only increases the shot noise by contributing to higher dark current but more importantly, it also introduces additional frequency dependent noise (potentially *1/f* noise), resulting in much higher noise in the detector. The 1/*f* noise has been extensively studied in p-n junctions. In particular, in MCT photodiodes, 1/*f* noise has been often associated with modulation of the surface generation currents induced by fluctuations of the surface potential. While the mechanisms of the surface leakage current in the Sb-based SL photodiodes are not completely understood yet, evidently the surfaces current can be a source of extraneous noise in these devices similar to MCT detectors. Since strong frequency-dependent noise can be generated by sidewall leakage current, it is important to fabricate the high performance SL detectors and focal plane array (FPA) using the technology that can minimize the mesa side-wall leakage current. One way to achieve this result is by development of reliable sidewall passivation that can suppress the leakage current and prevent the onset of frequency-dependent noise. More details of these noise and gain studies can be found in Reference 13.

We have also developed a dry-etch technique for pixel isolation for achieving low surface leakage for LWIR superlattice detectors. The surface leakage was reduced through the etching mechanism by minimizing the amount of differential etching and removing unwanted native oxides, byproducts, and contaminants on the sidewalls. The advantages to both chlorine-based and methane-based plasmas were exploited and combined to achieve over two orders of magnitude improvement in dark current compared to diodes etched with BCl_3/Ar. Each gas in $CH_4/H_2/BCl_3/Cl_2$/Ar etch governed its own unique role in minimizing surface leakage. CH4/H2 forms a thin polymer layer that serves as a passivant and protectant while sustaining near-vertical sidewalls and allowing for lower-temperature etches due to its volatility. BCl_3 effectively removes native oxides that contributes to the surface potential, and Cl_2 was added to increase the etch rate and prevent mask erosion. Effectively utilizing the proper gas ratios and etch parameters, differential etching was eliminated and thus avoided ripples in the sidewalls, a source for electrically active sites. This etch technique was proven to achieve dark currents as low as wet etching while significantly improving fill factor and uniformity. Near-vertical, smooth sidewalls with minimal dielectric mask erosion were achieved with good anisotropy resulting in more than three times higher fill factor. These performance enhancements allow small pixel size, large format LWIR FPAs to become more realizable. More details of the dry-etch technique can be found in Reference 14.

3. CBIRD FOCAL PLANE ARRAY DEVELOPMENT

This high-performance CBIRD device reported in Reference 11 has an N-p junction near the top surface. It collects electrons at the detector top contact and requires an n-on-p (or top positive polarity) read out integrated circuit (ROIC). The most commonly available ROICs are for p-on-n devices, which would need to operate with a reversed CBIRD device structure that collects holes from the top. We call the top electron and hole collecting devices n-CBIRD and p-CBIRD, respectively. We have grown both n-CBIRDs and p-CBIRDs on GaSb wafers. The epitaxially grown material was processed into 200 μm diameter mesa photodiode test structures using dry etch processing. Structurally the p-CBIRD is the n-CBIRD grown in reverse order, and thus should have very similar I-V characteristics. However, while the reverse-bias I-V characteristic of the n-CBIRD appears nearly diffusion limited, the p-CBIRD clearly is not. One

possible explanation the observed difference is dopant migration. Nominally, the pN junction is at the absorber/hB SL interface. In the n-CBIRD, during growth, p dopants in the absorber can migrate into the hB SL grown on top of it, moving the junction into the wider gap hB SL. The opposite happens in the p-CBIRD, placing the junction in the narrow gap absorber region, which facilitates trap-assisted tunneling processes.

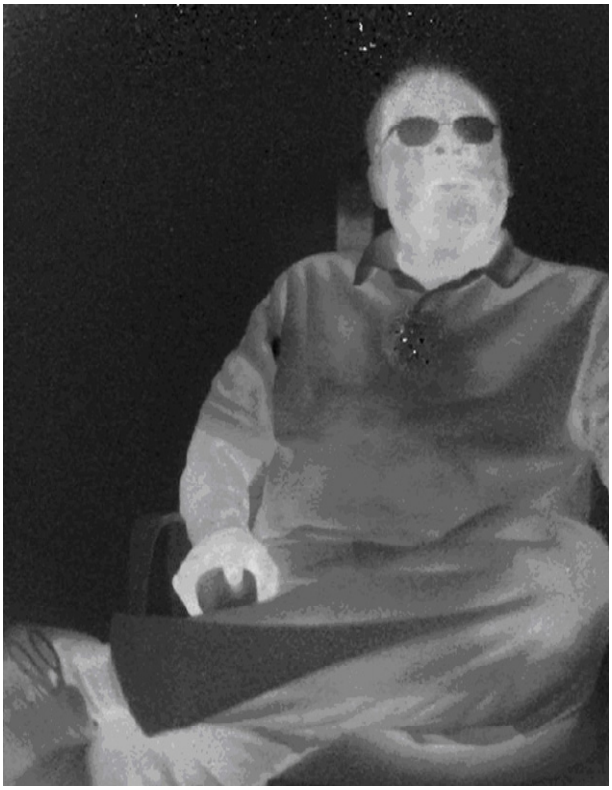

Figure 2. An image taken with the LWIR p-CBIRD FPA

1024x1024 pixel detector arrays with 19.5 μm pixel pitch were fabricated by dry etching through the top contact, eB SL, and photosensitive absorber SL, into the detector common layer (i.e., hB SL). The dry etching was done using an inductively coupled plasma (ICP) system using a combination of gases: CH4/H2/BCl3/Cl2/Ar. Ohmic contact metal was evaporated and unwanted metal was removed using a metal lift-off process. The actual pixel size is 17.5x17.5 μm^2 with 81% fill factor. Five detector arrays were processed on a four-inch GaSb wafer with etch rate uniformity better than 5% across the array. Indium bumps were then evaporated on top of the detectors for hybridization with ROICs. Several LWIR SL detector arrays were chosen and hybridized to 1024x1024 pixel direct injection silicon ROICs.

A selected 1Kx1K LWIR p-CBIRD FPA on a LLC was installed into a liquid nitrogen pour filled test dewar with f/2 cold-stop. At temperatures below 80 K, the signal-to-noise ratio of the system is limited by the measurement noise of the measurement setup. This initial array has a pixel operability of 96.3%. The measured FPA quantum efficiency is 21%. The cutoff wavelength is 11.5 μm. The noise equivalent differential temperature (NEΔT) of 53 mK was obtained at an operating temperature of 80 K, with 300 K background and cold-stop. An image taken with the first megapixel LWIR p-CBIRD SL camera is shown in Figure 2. The p-CBIRD FPA is reported in more detail in Reference 15. Also, we have fabricated a 320×256 format FPA based on the n-CBIRD design. Figure 3 shows an image taken with this FPA at an operating temperature of 78K. The 50%-responsivity cutoff wavelength for this array is 10 μm. Preliminary analysis indicates an operability of 98%, and an NEΔT of 26 mK with 300 K background.

4. CONCLUSIONS

The antimonide material system is relatively robust and has the potential for good manufacturability. The versatility of the material system, with the availability of three different types of band offsets, provides great flexibility in device design. In the MWIR, the use of unipolar barriers in the nBn design has already seen success. In the LWIR, type-II InAs/Ga(In)Sb superlattices have been shown theoretically to have reduced Auger recombination and suppressed band-to-band tunneling. Suppressed tunneling allows for higher doping in the absorber, which has led to reduced diffusion dark current. Heterostructures such as those based on the CBIRD design have been used effectively to suppress G-R dark current. As a result, the dark current performance of antimonide superlattice based single element LWIR detectors are now approaching that of the state-of-the-art MCT detector, with sufficient performance for tactical applications and potential for strategic applications [16]. To date, the antimonide superlattices still have relatively short carrier lifetimes; this issue needs to be resolved before type-II superlattice infrared detectors can achieve their true potential. Reliable surface leakage current suppression methods, such as that based robust surface passivation, would be needed to achieve high-performance in focal plane arrays. Preliminary focal plane arrays results are highly encouraging.

Figure 3. Images taken with a 320×256 format LWIR n-CBIRD focal plane array at an operating temperature of 78K. The detector cutoff wavelength is 10 μm.

5. ACKNOWLEDGEMENT

The authors thank Dr. M. Tidrow, Dr. S. Bandara, and Dr. L. Zheng for encouragement and support. The research described in this publication was carried out at the Jet Propulsion Laboratory, California Institute of Technology, under a contract with the National Aeronautics and Space Administration. This work was sponsored by the Missile Defense Agency.

REFERENCES

[1] G. A. Sai-Halasz, R. Tsu, and L. Esaki, "A new semiconductor superlattice," *Appl. Phys. Lett.* **30**(12), 651-653 (1977).

[2] C. H. Grein, P. M. Young, and H. Ehrenreich, "Minority carrier lifetimes in ideal InGaSb/InAs superlattices," *Appl. Phys. Lett*. **61**(24), 2905 (1992).

[3] E. R. Youngsdale, J. R. Meyer, C. A. Hoffman, F. J. Bartoli, C. H. Grein, P. M. Young, H. Ehrenreich, R. H. Miles, and D. H. Chow, "Auger lifetime enhancement in InAs-$Ga_{1-x}In_xSb$ superlattices," *Appl. Phys. Lett.* **64**(23), 3160-3162 (1994).

[4] D. L. Smith and C. Mailhiot, "Proposal for strained type II superlattice infrared detectors," *Appl. Phys. Lett.* **34**(10), 663-665 (1987).

[5] D. L. Smith, T. C. McGill, and J. N. Schulman "Advantages of the HgTe-CdTe superlattice as an infrared detector material," *Appl. Phys. Lett.* **43**(2), 180-182 (1983).

[6] F. Fuchs, J. Wagner, J. Schmitz, N. Herres, and P. Koidl, "Growth and Characterization of InAs/AlSb/GaSb Heterostructures." in *Antimonide-related strained-layer heterostructures* (M. O. Manasreh, Ed.), pp. 191-232. Gordon Breach Science Publishers, Amsterdam (1997).

[7] L. Bürkle and F. Fuchs, "InAs/(GaIn)Sb superlattices: a promising material system for infrared detection" in *Handbook of Infrared Detection Technologies* (M. Henini and M. Razeghi, Ed.), pp. 159-189. Elsevier Science, Oxford (2002).

[8] L. Bürkle and F. Fuchs, "GaSb/InAs superlattices for infrared FPAs" in *Handbook of Infrared Detection Technologies* (M. Henini and M. Razeghi, Ed.), pp. 191-232. Elsevier Science, Oxford (2002).

[9] David Z.-Y. Ting, Alexander Soibel, Linda Höglund, Jean Nguyen, Cory J. Hill, Arezou Khoshakhlagh, and Sarath D. Gunapala, "Type-II Superlattice Infrared Detectors" in *Semiconductors and Semimetals*, Vol. 82, *Advances in Infrared Photodetectors* (S. Gunapala, D. Rhiger, and C. Jagadish, Ed.), Elsevier (2011).

[10] A. Rogalski, *Infrared Detectors*, CRC Press, Boca Raton (2011).

[11] D. Z.-Y. Ting, C. J. Hill, A. Soibel, S. A. Keo, J. M. Mumolo, J. Nguyen, and S. D. Gunapala, "A high-performance long wavelength superlattice complementary barrier infrared detector," *Appl. Phys. Lett*. **95**, 023508 (2009).

[12] Linda Höglund, Alexander Soibel, Cory J. Hill, David Z. Ting, Arezou Khoshakhlagh, Anna Liao, Sam Keo, Michael C. Lee, Jean Nguyen, Jason M. Mumolo, Sarath D. Gunapala, "Optical studies on antimonide superlattice infrared detector material", *Proc. SPIE* **7780**, 77800D (2010).

[13] Alexander Soibel, David Z.-Y. Ting, Cory J. Hill, Mike Lee, Jean Nguyen, Sam A. Keo, Jason M. Mumolo, and Sarath D. Gunapala, "Gain and noise of high-performance long wavelength superlattice infrared detectors", *Appl. Phy. Lett.* **96**(11), 111102 (2010).

[14] Jean Nguyen, Alexander Soibel, David Z.-Y. Ting, Cory J. Hill, Mike C. Lee, and Sarath D. Gunapala, "Low dark current long-wave infrared InAs/GaSb superlattice detectors", *Appl. Phy. Lett.***97**(5), 051108 (2010).

[15] S. D. Gunapala, D. Z. Ting, C. J. Hill, J. Nguyen, A. Soibel, S. B. Rafol, S. A. Keo, J. M. Mumolo, M. C. Lee, J. K. Liu, and B. Yang, "Demonstration of a 1024 1024 Pixel InAs–GaSb Superlattice Focal Plane Array", *IEEE Photonics Technol. Lett.* **22**(24) 1856-1858 (2010).

[16] Sumith V. Bandara, "Performance Analysis of InAs/Ga(In)Sb Strained Layer Superlattice Detectors and Focal Plane Arrays", *Proc. of SPIE* **7608**, 76081M (2010).